

NUMERICAL INVESTIGATIONS OF TERRAIN VEHICLE TIRE SUBJECTED TO BLAST WAVE

Paweł Baranowski, Jerzy Małachowski

*Military University of Technology, Faculty of Mechanical Engineering
Department of Mechanics and Applied Computer Science
Gen. Sylwestra Kaliskiego Street 2, 00-908 Warsaw, Poland
tel.: +48 22 6839654, fax: +48 22 6839355
e-mail: pbaranowski@wat.edu.pl, jerzy.malachowski@wat.edu.pl*

Abstract

In this paper a numerical model of a terrain vehicle suspension system development process is presented. In the performed studies the suspension system with and without a simplified motor-car body was taken into consideration. Geometry of the tire, wheel and system elements were achieved using reverse engineering technology. Moreover, with the assistance of a microscope and an X-ray device it was possible to achieve the exact tire cords pattern, which in the next stages was implemented into the FE model. Subsequently, numerical simulations of both cases were performed simulating the TNT explosion under a wheel. The non-linear dynamic analyses were performed using the LS-DYNA code. To solve both presented cases the explicit central difference scheme with modified time integration of the equation of motion was implemented. Computations of blast wave propagation were carried out with the Smooth Particle Hydrodynamics (SPH) method with Jones Wilkins Lee (JWL) equation of state defining the explosive material. Obtained results have shown different suspension system elements damage and tire destruction characteristic, which come from blast wave reflection of the motor-car body surface.

Keywords: blast wave, Finite Element Analysis, SPH, JWL, tire, vehicle suspension system, vehicle suspension

1. Introduction

Improvised Explosive Devices (IED), apart from other “tools of destruction”, are the most commonly used explosive devices in the ongoing world military conflicts. Its destructive effect manifests in a tire tearing apart followed by large deformation of other suspension system elements. Moreover, formed blast wave reverberates from motor-car body bottom surface instead of dissipating. Reflected blast wave interacts with suspension elements dealing more overall damage to vehicle chassis.

The authors of the paper have decided to carry out numerical computations of an explosion under the terrain vehicle with the blast wave reflection effect taking into account. The main objective was to examine a destructive mechanism of a blast detonation process, as presented in the other literature [1,2,3].

With the explosion phenomenon exothermic reactions, induced by external effects, are produced. These reactions result in mechanical work through the evolution of highly compressed hot gasses. Gas products which fills the explosive material are compressed at the surface and, combined with the surrounding medium, generate an abrupt growth of a pressure.

Additionally, in the overall explosion process extremely significant is the velocity of the blast wave propagation reaching values between 1000-10000 m/s. These fundamental factors, e.g.: gas products, high reaction rate and exothermic effects have the biggest influence on how the detonation proceeds and what destruction it would have. In Figure 1 an exemplary damaged vehicle is presented [4].

In order to model the detonation process of high explosive material numerical computations were performed based on the SPH (Smooth Particle Hydrodynamics) method. In presented

investigations the suspension system with and without a simplified motor-car body was taken into consideration.



Fig. 1. Military vehicle "Cougar" after mine explosion [4]

2. Object of investigation

In the presented paper numerical model of the suspension system was developed based on the real off-road vehicle chassis elements. The major suspension system parts are: longitudinal, spring, axle, axle bush, hub, drum brake, drum brake pads, steel rim and wheel. Geometry of the tire and other suspension elements was achieved thanks to the reverse engineering technology. Since the authors expected that destructive process of the analysed structure will initiate in the vehicle wheel they decided to describe it accurately. Hence the tire wheel was divided into six different parts, with corresponding material properties, as presented in the previous literature [5,6,7]. Moreover, with the assistance of a microscope and an X-ray device it was possible to achieve the exact tire cords pattern, which in the next stages was implemented into the FE model (Fig.2).

In the performed studies the suspension system with and without a motor-car body was taken into consideration. The motor-car body was represented by simplified surface modelled with 11266 shell elements and 11455 nodes with 25% of vehicle mass associated. The FE model of suspension system reached 59633 solid and beam elements and 87108 nodes.

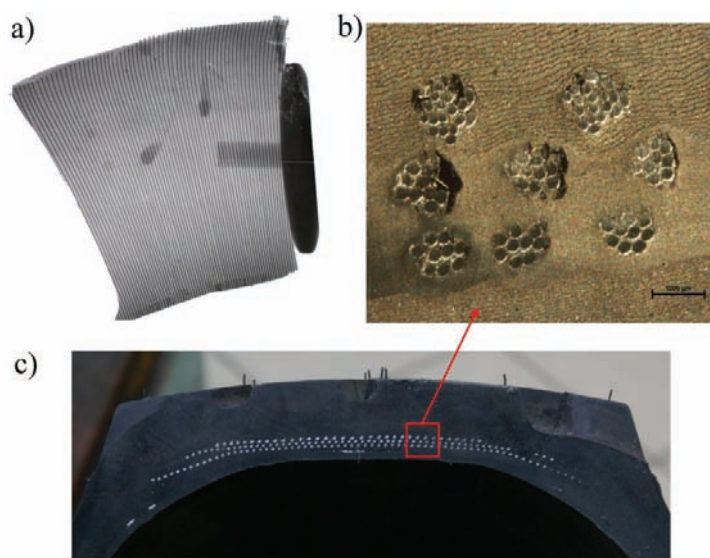


Fig. 2. a) X-ray photography of cords pattern in tire sidewall, b) Tread cords pattern in microscale, c) Cords pattern in tire tread

Due to the fact that a tire is such a complex structure to be represented with numerical methods, it was important to develop a discrete model of it as much similar to the real one as possible. Table 1 presents the suspension system parts statistic data, whereas in Table 2 the statistic data of the tire is presented. The main steel components in the tire were modelled using nonlinear mechanical properties. The other rubber components were described with nonlinear model based on the Mooney-Rivlin constitutive equation [8]. Geometrical representation of the analysed discrete model is presented in Figure 3.

Tab. 1. Statistic data of discrete suspension system model

Part	No. of elements (HEX8)	No. of nodes	Material model
<i>Tread</i>	3840	6360	Rubber
<i>Inner fabric</i>	3600	7680	Rubber
<i>Carcass</i>	1680	3600	Rubber
<i>Sidewall</i>	4800	8160	Rubber
<i>Bead core</i>	2400	3840	Rubber
Part	No. of beam elements	Nodes	Material Model
<i>Circumferential cords</i>	4560	4561	Steel
<i>Radial cords</i>	8639	8881	Steel

Tab. 2. Statistic data of discrete tire model

Part	No. of elements (HEX8)	No. of nodes	Material model
<i>Tire</i>	16320	25520	Rubber/Steel
<i>Rim</i>	7192	12164	Steel
<i>Drum brake</i>	4680	7440	Cast iron
<i>Axle</i>	4278	5236	Steel
<i>Hub</i>	2268	3132	Steel
<i>Axle bush</i>	4585	6207	Steel
<i>Spring</i>	4368	7077	Steel
<i>Longitudinal</i>	7302	9052	Steel
Part	No. of elements (Shell)	No. of nodes	Material model
<i>Motor-car body</i>	11266	11455	Steel

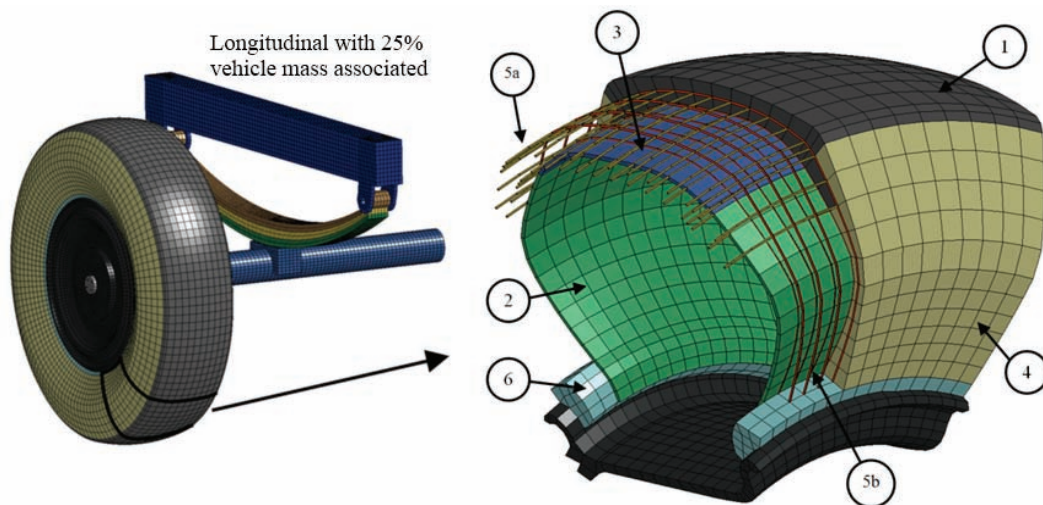


Fig. 3. FE suspension system model and tire components (1. Tread, 2. Inner fabric, 3. Carcass, 4. Sidewall, 5a. Circumferential cords, 5b. Radial cords, 6. Bead core with cords)

3. Numerical Tests Description

3.1. Boundary initial conditions

Suspension system loaded with a blast wave was modelled with one of the techniques available in LS-Prepost/LS-Dyna software [9], e.g.: Smoothed Particle Hydrodynamics method. In the performed studies the suspension system with and without a simplified motor-car body was taken into consideration. In order to minimize the computation time only one wheel and 1/4 of the vehicle body was modelled with symmetry conditions. Pressure inside a tire was represented by the airbag model (Green function closed volume integration) [9]. For numerical tire destruction the erosion criteria was implemented based on the effective strain failure variable. Preliminary tests were carried out with the total charge mass of 2 kg situated at the distance of 0,3 m under the wheel displaced with 0,3 m toward the end of axle (Fig. 4). The explosive charge was modelled with 300000 SPH particles, which was necessary to reflect a hydrodynamic behaviour of the blast wave propagation. In order to reduce the computation time, a box envelope was specified, within which SPH particles approximations are computed. This eliminates particles that are no longer interacting with the suspension system. Consequently, the results of both analyses were compared.

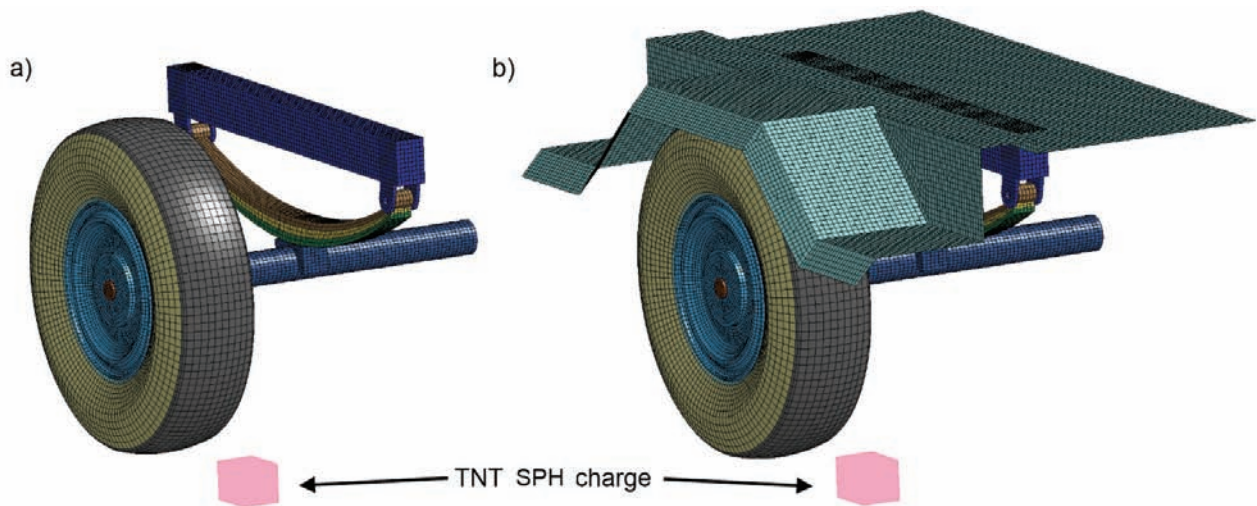


Fig. 4. SPH TNT charge placement for a) suspension system without vehicle body, b) suspension system with motor-car body

3.2. SPH blast technique

It is a meshless particle method with Lagrangian nature, where computational information including mass and velocity are carried with particles. The main difference between classical methods and SPH is the absence of a grid. Therefore, those particles are the framework on the region within the governing equations are solved [9]. SPH method uses the concept of kernel and particle approximation as follows [9]:

$$\Pi^k f(x) = \int f(y)W(x-y, h)dy \quad (1)$$

where: W is the kernel function, which is defined using the function (θ) by the relation:

$$W(x, h) = \frac{1}{h(x)^d} \theta(x) \quad (2)$$

where: d is the number of space dimensions and h is the so-called smoothing length which varies in time and in space.

3.3. Jones Wilkins Lee equation of state

In order to model the explosion with SPH, it was significant to define the material with Jones Wilkins Lee (JWL) equation of state [10]:

$$p = A \left(1 - \frac{\omega}{R_1 \bar{\rho}} \right) \exp \left(-R_1 \bar{\rho} \right) + B \left(1 - \frac{\omega}{R_2 \bar{\rho}} \right) \exp \left(-R_2 \bar{\rho} \right) + \frac{\omega \bar{e}}{\bar{\rho}}, \quad (3)$$

where: $\bar{\rho} = \frac{\rho_{he}}{\rho}$ is density of products of detonation (PD); $e = \rho_{he} e$ is specific internal energy of PD; ρ_{he} refers to density of the high explosive (HE); p represents pressure of PD; A, B, R_1, R_2, ω are empirical constants determined for the specific type of HE.

Table 3 includes values of the mentioned constants found in the JWL equation [10] for the TNT used for the computations.

Tab. 3. TNT constants for the JWL equation of state [10]

Material	P [kg/m ³]	A [Pa]	B [Pa]	R1 [-]	R2 [-]	ω [-]
TNT	1630	3.712e+11	3.231e+9	4.150	0.950	0.3

3.4. Numerical solution

To solve both presented cases the explicit central difference scheme with modified time integration of the equation of motion was implemented. In this method an acceleration and velocity at time t are given by [11]:

$$\ddot{q}_t = \frac{1}{(\Delta t)^2} [q_{t-\Delta t} - 2q_t + q_{t+\Delta t}], \quad (4)$$

$$\dot{q}_t = \frac{1}{2\Delta t} [q_{t+\Delta t} - q_{t-\Delta t}]. \quad (5)$$

where: $q_t, (\dot{q}_t, \ddot{q}_t)$ is the value of a function $q(\tau), (\dot{q}(\tau), \ddot{q}(\tau))$ at time $\tau = t, \tau \in [t_0, t_s]$.

The semi-discrete matrix equation of motion for the nonlinear case at time t is [11]:

$$\left[\frac{1}{(\Delta t)^2} M + \frac{1}{2\Delta t} C \right] q_{t+\Delta t} = F_t - \left[K - \frac{1}{(\Delta t)^2} M \right] q_t - \left[\frac{1}{(\Delta t)^2} M - \frac{1}{2\Delta t} C \right] q_{t-\Delta t}, \quad (6)$$

where: M is the global mass matrix, C is the global damping matrix, F is the global load matrix, K is the global stiffness matrix.

To achieve stability of computations the authors needed to meet the Courant-Friedrichs-Lewy (CFL) condition which states that a necessary condition for the convergence of an explicit finite difference scheme is that the domain of dependence of the discrete problem includes the domain of dependence of the differential equation in the limit as the length of the finite difference steps goes to zero.

4. Numerical tests results comparison

As results from the carried out analyses the tire destruction was obtained. The response of the vehicle chassis structure to the SPH blast loading is presented in Figure 5. Graph presented in Figure 6 describes the velocity change over time of one of the reflected SPH particle.

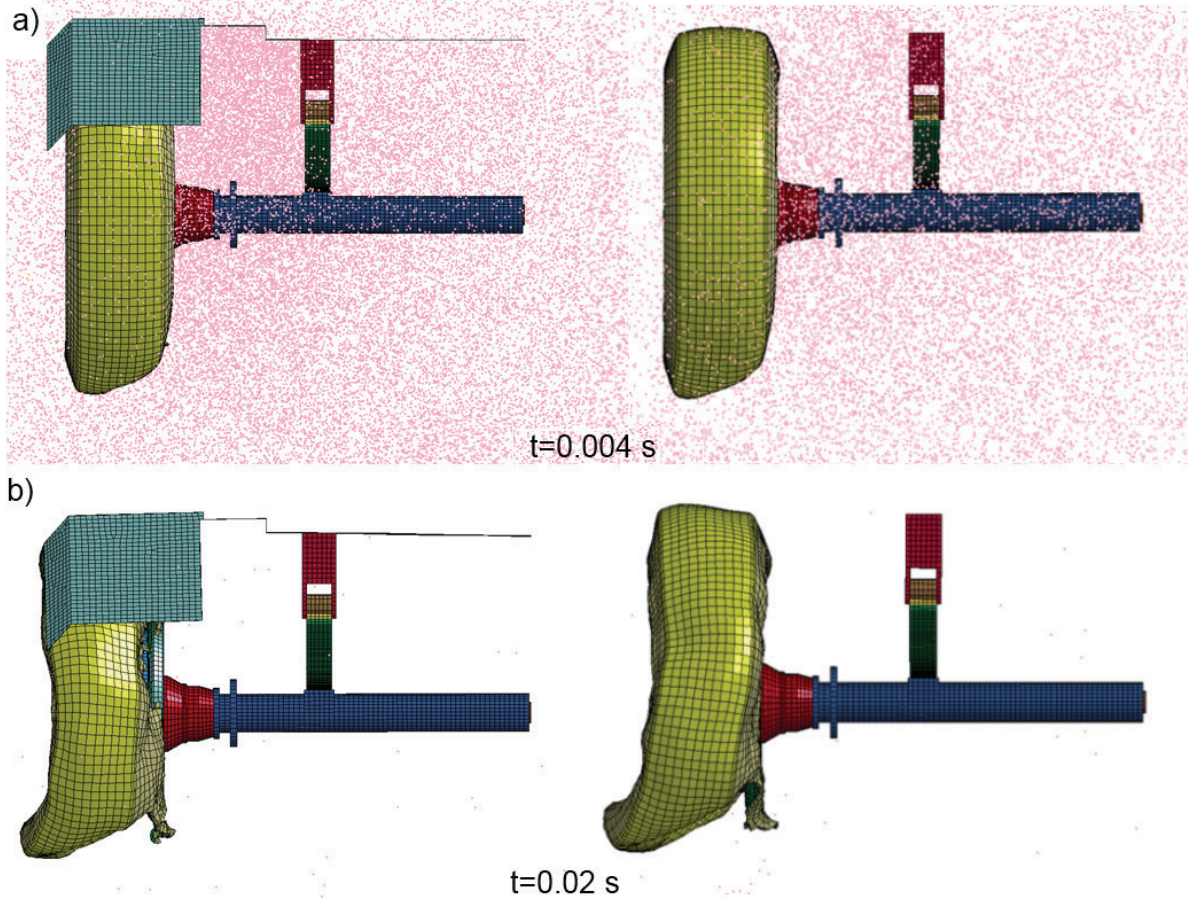


Fig. 5. SPH particles interacting with the suspension system structure: results comparison

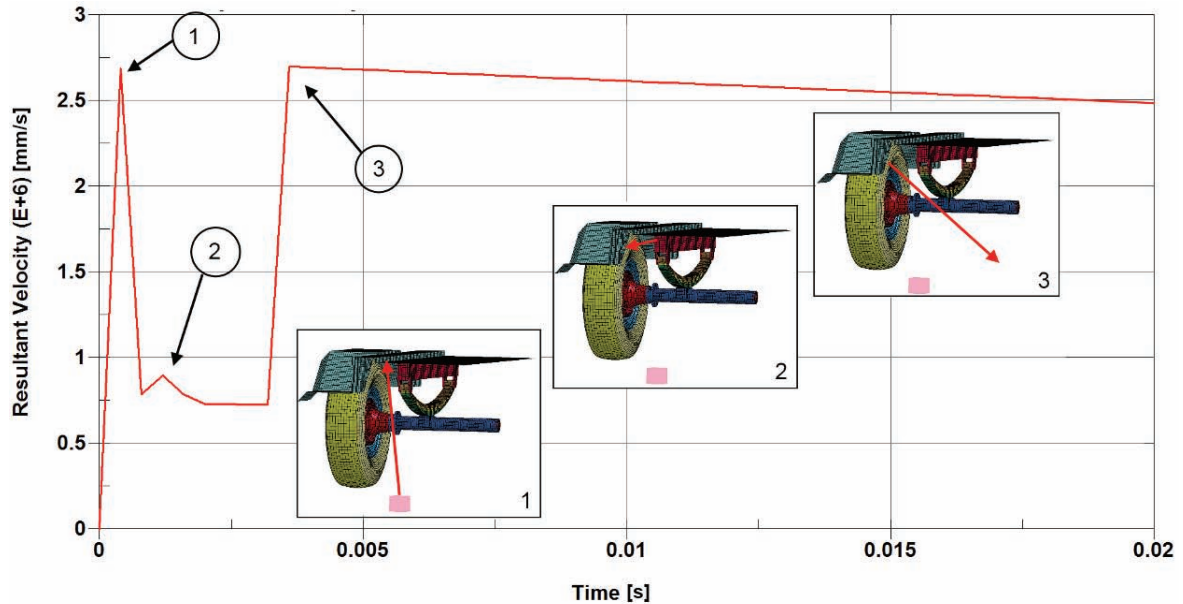


Fig. 6. Resultant velocity versus time of the selected SPH particle

The comparison of tire destruction for both cases is presented in Figure 7. It can be seen that in the numerical simulation of suspension system with simplified motor-car body blast wave reflects from its surface and deals more damage to vehicle chassis elements. Moreover, reverberated particles (conventionally representing pressure wave) interact with the tire which results not only in destruction of the tire bottom structure but also in upper side of it. Thus this means that more internal energy is absorbed by the tire, what can be noticed in Figure 8. The visible difference in

presented plots also derives from the hourglass effect which can be explained as non physical behaviour of discrete elements

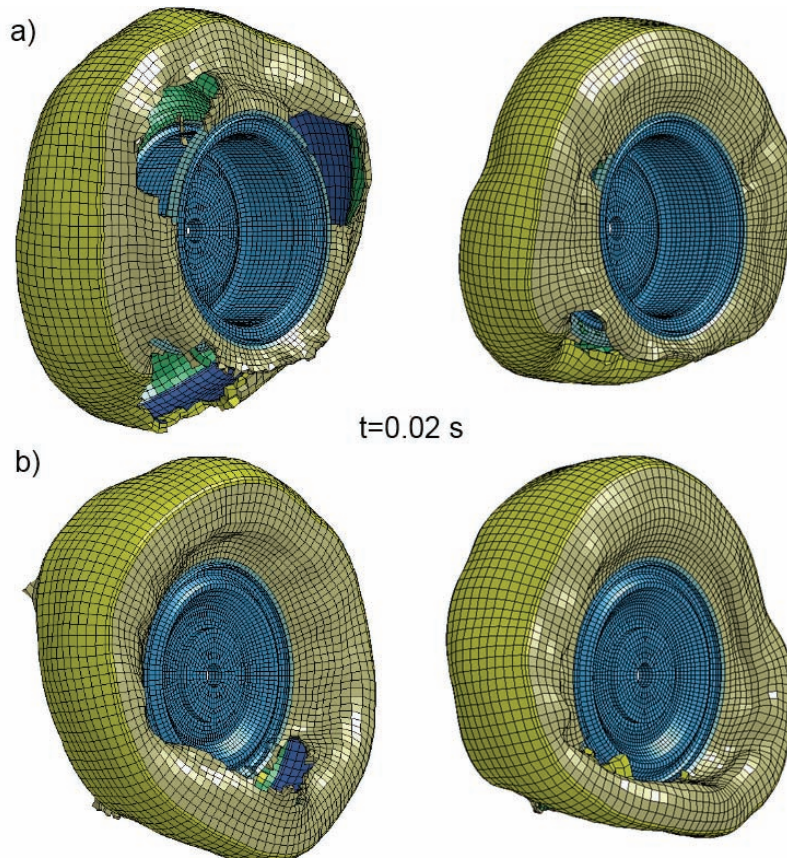


Fig. 7. Tire destruction at $t=0.02$ s, a) Inner side of rim, b) Outer side of rim (left: suspension with motor-car body, right: suspension without motor-car body)

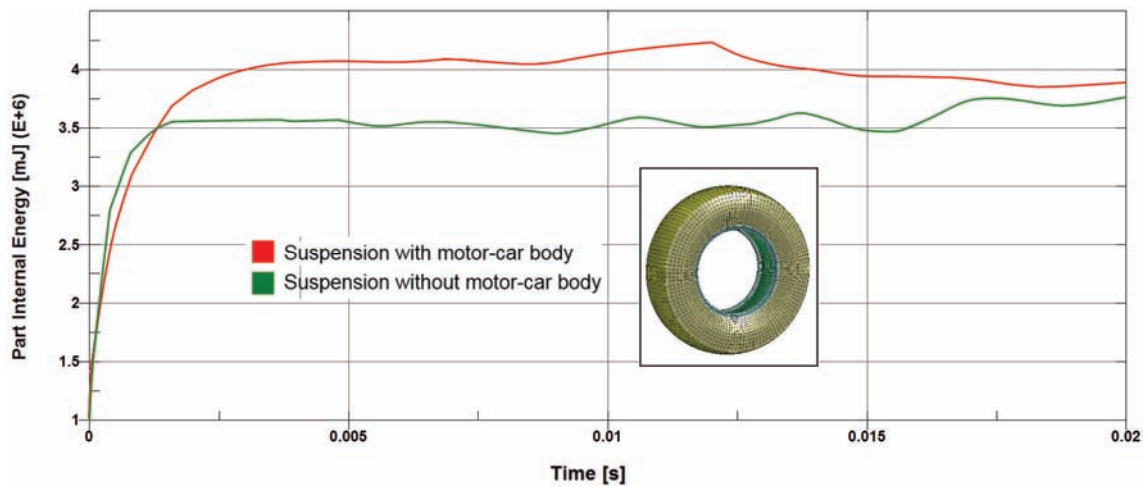


Fig. 8. Tire internal energy graph for both cases

5. Conclusions

The authors of the presented paper made an attempt of simulating the vehicle suspension system with and without motor-car body subjected to the blast wave modelled with SPH particles. Numerical computations have been carried out in order to investigate the response of the suspension system structure. Performed analyses have completely confirmed destructive effect of

the explosion under the vehicle chassis. From the obtained results it can be noticed that the most devastated element of the examined suspension system is the tire. It consumes the most of the detonation energy which results in its destruction.

Moreover, it can be seen that in the numerical simulation of suspension system with simplified motor-car body blast wave reflects from its surface and deals more damage to vehicle chassis elements. This results not only in destruction of the tire bottom structure but also in upper side of it. Proposed blast modelling confirms its effectiveness in simulation of TNT or IED explosion of such a complex structure as a tire. Nevertheless, analyses have shown the low tire resistance which in the further work will be investigated in order to improve its durability to a shock wave. The explosion will be simulated with some improvements in the tire, e.g. with a ring inside it. Additionally, in the numerical modelling the influence of the soil will be tested which will be simultaneously verified in field tests.

References

- [1] Morka, A., Kwaśniewski, L., Wekezer, J., *Assessment of Passenger Security in Paratransit Buses*, Journal of Public Transportation, vol. 8, pp. 47-63, 2005.
- [2] Lacombe, J.L., *Analysis of Mine Detonation, SPH analysis of structural response to anti-vehicles mine detonation*, LSTC 2007.
- [3] Toussaint, G., Durocher, R., *Finite Element Simulation using SPH particles as loading on typical light armoured vehicles*, 10th International LS-Dyna Users Conference.
- [4] <http://en.wikipedia.org/wiki>.
- [5] Neves, R.R.V., Micheli, G.B., Alves, M., *An experimental and numerical investigation on tyre impact*, International Journal of Impact Engineering, vol. 10, pp. 685-693, 2010.
- [6] Cho, I.R., Kim, K.W., Jeong, H.S., *Numerical investigation of tire standing wave using 3-D patterned tire model*, Journal of Sound and Vibration, vol. 305, pp. 795-807, 2007.
- [7] Pondel, B., Małachowski, J., *Numeryczna analiza pracy opony samochodowej*, WAT, Warszawa 2006.
- [8] Helnwein, P., Liu, C.H., Meschke, G., Mang, H.A., *A new 3-D finite element model for cord-reinforced rubber composites- application to analysis of automobile tyres*, Finite Elements in Analysis and Design, vol. 4, pp. 1-16, 1993.
- [9] Hallquist, J.O., *LS-Dyna. Theory manual*, California Livermore Software Technology Corporation (1998).
- [10] Małachowski, J., *Modelowanie i badania interakcji ciało stałe-gaz przy oddziaływaniu impulsu ciśnienia na elementy konstrukcji rurociągu*, BEL Studio, Warszaw, 2010.
- [11] Dacko, M., Borkowski, W., Dobrociński, S., Niezgoda, T., Wieczorek, M., *Metoda elementów skończonych w mechanice konstrukcji*, Arkady, Warszawa 1994.